Structure and Phase Transitions of Poly(diethylsiloxane)

Aart Molenberg and Martin Möller*

University of Ulm, Organische Chemie III/Makromolekulare Chemie, 89069 Ulm, Germany

Received June 3, 1997; Revised Manuscript Received September 29, 1997[⊗]

ABSTRACT: Phase transitions and morphology of poly(diethylsiloxane) have been studied with help of differential scanning calorimetry and transmission electron microscopy on carbon−platinum replicas of freeze-fractured samples. The TEM experiments showed distinct lamellae in the case of the β and γ crystalline polymorphs, whose thicknesses correlated well with the calculated chain lengths, demonstrating an extended chain conformation for both polymorphs. A low heating rate dependence of the $\beta \rightarrow \mu$ transition temperature in DSC and a linear relationship between isotropization temperature and reciprocal molecular weight indicated the existence of extended chain lamellae for the mesophase as well. The α crystalline polymorph displayed a greater softness than β- and γ-PDES, and no lamellar structures could be observed. DSC experiments on bimodal mixtures of PDES samples with strongly different molecular weights demonstrated molecular weight dependent phase separation in the case of β-PDES and the occurrence of mixed lamellae for the mesophase obtained from α-PDES. For the latter, a less ordered packing with chain ends incorporated into the lamellae was proposed. Upon heating γ-PDES no mesophase was formed, which was explained by surface energy effects. The critical molecular weight for mesophase formation was found to be $M_n = 28\,000$ g/mol.

Introduction

Poly(diethylsiloxane) (PDES) is the first member of a series of poly(di-*n*-alkylsiloxane)s that are able to form a mesophase.[1−5] Regarding the conformational disordering, this mesophase has been described as a *condis* phase;[6,7] regarding the two-dimensional ordering, it can be compared to columnar discotic phases.[8]

When cooled below the mesophase, high molecular weight PDES has been shown to crystallize into two different modifications: α- and β-PDES.[1−3] The thermodynamically more stable β phase is formed preferably upon slow cooling from the mesophase (μ), whereas a high fraction of α-PDES is obtained upon fast cooling. X-ray diffraction data have demonstrated a monoclinic packing of α-PDES and a tetragonal lattice in the case of β-PDES.[2,3] Electron micrographs obtained from carbon−platinum replicas of freeze fractured surfaces hinted toward a chain folded morphology in α-PDES and extended chain crystallization in β-PDES,[7] but were not fully unambiguous. A third crystalline modification has been reported for low molecular weight PDES[10−12] and quenched samples of high molecular weight.[1] This modification, designated γ-PDES, was found to be thermodynamically less stable than the α modification and closely resembles the tetragonal β modification.[11,12]

^{1}H solid state NMR,[13−15] ^{2}H solid state NMR,[16] ^{13}C solid state NMR,[4,17] ^{29}Si solid state NMR,[4,9,17,18] Raman spectroscopy,[19] dielectric relaxation measurements,[9,20] and molecular mechanics calculations[21] indicated the onset of jumplike motions of the ethyl groups and restricted librations of the −Si−O− backbone at the transition from the low-temperature to the high-temperature crystalline phase. The transition into the mesophase is characterized by the onset of large amplitude molecular mobility of the backbone. Whereas conformational disordering is restricted to the alkyl side chains in the less disordered high temperature crystal, in the mesophase the inorganic backbone is disordered as well. Two states of molecular mobility have been observed in the mesophase by solid state ^{1}H NMR experiments.[22] These locally ordered and locally defect-enriched states were in dynamic equilibrium with mean exchange times varying between 0.1 and 1 s in the temperature range of the mesophase.

On the basis of the comparison of the theoretical crystallographic density and the experimentally determined density,[2] a monoclinic lattice has been proposed for the mesophase, which differs only slightly from the hexagonal columnar packing. Polarization microscopy has revealed that the mesophase grows from the melt in the form of lamellar domains with a thickness in the micrometer range, in which the polymer chains lie perpendicular to the end faces.[23] On account of the high order in the mesophase, an extended conformation was proposed for the polysiloxane chains.[3,23] Small angle neutron scattering experiments[10] have confirmed this hypothesis, i.e. in the mesophase the polymer chains are stretched in a rod-like conformation. The mesophase morphology of PDES shows analogy to that of polyethylene under high pressure. In the latter case, crystallization was proposed to initially occur in a folded-chain fashion, followed by rapid chain extension through sliding of the polymer chains along each other.[24]

This paper describes a new study on the molecular weight dependence of the thermal transitions of PDES. Two major questions are addressed. These are the remarkable molecular weight dependence of the transition from the mesophase to the isotropic melt, reported before,[3,10] and the question whether the thickness of the crystal lamellae can be correlated to the molecular weight of the PDES chains. For this purpose a series of PDES samples with narrowly distributed molecular weights have been prepared by anionic ring opening polymerization.[25] These samples and bimodal mixtures thereof were characterized by differential scanning calorimetry (DSC) and transmission electron microscopy (TEM). While the calorimetric experiments give evidence about the polymorphism, freeze-fracture TEM was used to evaluate the corresponding lamellar morphology in dependence of molecular weight and molecular weight distribution.

Experimental Section

Materials. Hexaethylcyclotrisiloxane (D_3^{Et}, where D^{Et} denotes a $-Si(Et_2)O-$ unit) was prepared as described before[26]

[⊗] Abstract published in *Advance ACS Abstracts,* December 1, 1997.

S0024-9297(97)00786-9 CCC: $14.00

Table 1. Molecular Weights and Transition Temperatures[a] and Enthalpies[b] for PDES Samples

sample no.	M_n[c]	M_w[c]	M_w/M_n[c]	M_w[d]	$T_{\gamma\to i}$ (°C)	$\Delta H_{\gamma\to i}$ (kJ/mol)	$T_{\alpha\to\mu}$ (°C)	$\Delta H_{\alpha\to\mu}$ (kJ/mol)	$T_{\beta\to\mu}$ (°C)	$\Delta H_{\beta\to\mu}$ (kJ/mol)	$T_{\mu\to i}$ (°C)	ΔH_i (kJ/mol)
1	11 800	13 100	1.11	14 300	−10.4	1.47	-		-		-	
2	23 700	25 800	1.09	30 000	−4.8	1.53	4.2		10.9		-	
3	27 900	32 200	1.15	42 100	−6.5		4.4		11.9		18.6	
4	40 200	44 000	1.10	55 600	-		5.1	1.82	12.1	2.02	28.3	0.28
5	66 700	74 000	1.12	89 100	-		6.5	1.72	14.8	2.13	39.0	0.33
6	95 900	111 000	1.16	137 000	-		6.5	1.82	15.0	2.17	42.0	0.35
7	112 000	139 000	1.25	175 000	-		7.0	1.74	15.5	2.22	44.9	0.36
8	143 000	189 000	1.31	262 000	-		6.8	1.58	15.3	2.25	46.2	0.35
9[e]	366 000	472 000	1.29	519 000	-		7.6	1.44	16.6	2.36	49.7	0.34
10[e]	430 000	596 000	1.39	669 000	-		7.9	1.52	17.0	2.23	51.1	0.33

[a] Peak temperatures, extrapolated to zero heating rate. Samples are cooled from the melt at 10 °C/min. [b] Upon heating at 10 °C/min. α-PDES was prepared by quenching from the melt, *β*-PDES by slow cooling and annealing above the melting point of the α phase. Isotropization enthalpies (ΔH_i) are obtained from samples which had been previously crystallized from the melt with 10 °C/min. [c] From GPC, polystyrene calibration. [d] From GPC, universal calibration. [e] Fractionated sample.

and purified by distillation from CaH_2 on a high vacuum line. The cryptand [211] (Merck, 98%) was distilled under high vacuum conditions, using a quartz apparatus. The ligand was obtained as a colorless liquid, which was dried azeotropically with toluene/$Mg(C_4H_9)_2$, dissolved in toluene, and stored under nitrogen in a quartz flask. Chlorotrimethylsilane (ABCR, 99.9%) and *sec*-BuLi (Aldrich, 1.3 mol/L in cyclohexane) were used as received.

Polymer Synthesis. Polymerizations were performed at ambient temperatures on a 10 g scale in bulk under a nitrogen atmosphere containing less than 1 ppm of H_2O and O_2. The initiator lithium *sec*-butyldiethylsilanolate (*sec*-BuSi(Et_2)OLi) was prepared in situ by addition of *sec*-BuLi to hexaethylcyclotrisiloxane (D_3^{Et}) and stirring overnight. Propagation was started by addition of a 2-fold excess of the lithium complexing cryptand [211] and terminated with chlorotrimethylsilane at about 50−80% D_3^{Et} conversion. Polymers were isolated from the reaction mixture, and purified by repeatedly precipitating in hot ethanol, and dried under vacuum at 80 °C.

Methods. Molecular weights and molecular weight distributions were obtained from GPC. The setup consisted of Waters *μ*-Styragel columns with pore sizes of 10^5, 10^4, 10^3, and 10^6 Å. Sample detection was performed by a Waters 410 differential refractometer and a Viscotek H502B differential viscometer, allowing universal calibration. Toluene was used as the eluent and the setup was calibrated with narrow polystyrene samples.

DSC measurements on PDES were made with samples of about 3−5 mg using a Perkin-Elmer DSC 7 system. The samples were heated at 20, 15, 10, and 5 °C/min, respectively, after being cooled from the melt at 10 °C/min. Transition temperatures are given as peak temperatures, extrapolated to zero heating rate. Water, gallium, and indium were used as calibration standards. Bimodal mixtures were prepared by dissolving two PDES samples with different molecular weights in toluene, after which the solvent was distilled off.

Transmission electron micrographs were recorded with a Philips EM 301 or EM 400 microscope operating at 80 kV in the bright field mode. *β*-PDES was prepared by crystallizing a sample of PDES from the mesophase at a rate of 1 °C/min, repeatedly followed by melting the residual α-PDES and cooling at 1 °C/min again. α-PDES was prepared by quenching a sample from the melt to −146 °C in liquid Freon-22 and *γ*-PDES was prepared by cooling a low molecular weight sample from the melt at a rate of 1 °C/min. The samples were freeze-fractured at −150 °C in a Balzers BAF 301 freeze-fracture apparatus, and the fracture surfaces were shaded with platinum at an angle of 45° (layer thickness ca. 2.5 nm) and carbon at 90° (ca. 25 nm). The thus-obtained replicas were separated from the polymer by repeatedly washing with toluene and transferred onto copper grids.

Results and Discussion

Polymer Synthesis. Several samples of PDES were synthesized by anionic ring opening polymerization of hexaethylcyclotrisiloxane, using cryptated lithium as counterion. As has been reported before,[25] this system enables the synthesis of PDES samples with a narrow molecular weight distribution, even at high conversion (>80%). However, when polymerizations were aimed at higher molecular weights (≥ ca. 6×10^5 g/mol), the obtained molecular weights became progressively lower than calculated and the molecular weight distributions became broader. In Table 1 molecular weights and transition temperatures and enthalpies of the samples used here are listed.

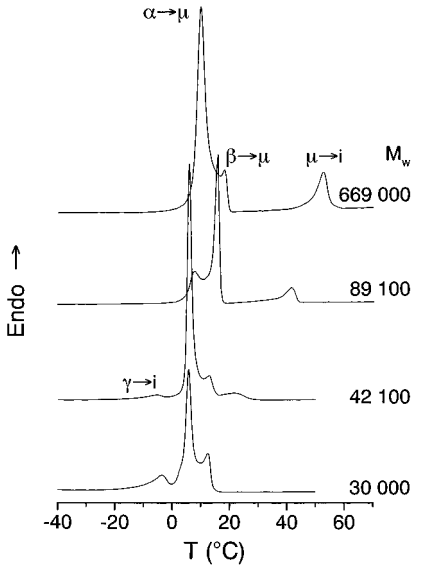

Figure 1. DSC heating scans for several PDES samples (heating rate 10 °C/min, after cooling from the melt with 10 °C/min).

Influence of Molecular Weight. Figure 1 shows DSC heating scans for a number of the samples that are listed in Table 1. Figure 2 represents a plot of the transition temperatures against the reciprocal molecular weight. The large molecular weight dependence of the isotropization temperature, even at the highest molecular weights, has been reported before as a rather unusual effect.[3,10]

A second important observation is that the mesophase is not formed below a critical molecular weight of M_n = 28 000, given by the intercept of the isotropization and the *β* to mesophase transition temperatures. Correspondingly, a mesophase could not be observed for the PDES sample with M_n = 27 500 (M_w = 30 000), either by DSC or by polarizing microscopy.

The molecular weight dependent destabilization of the mesophase comes along with the occurrence of another crystal modification, which has been denoted as *γ*-PDES:[10−12] if the molecular weight was lower than 50 000, a third transition emerged below the transitions of α- and

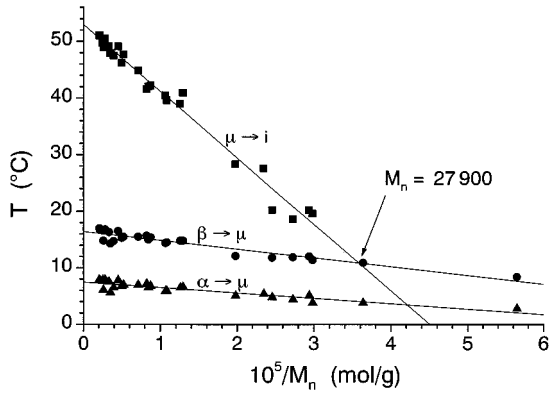

Figure 2. PDES transition temperatures vs reciprocal molecular weight.

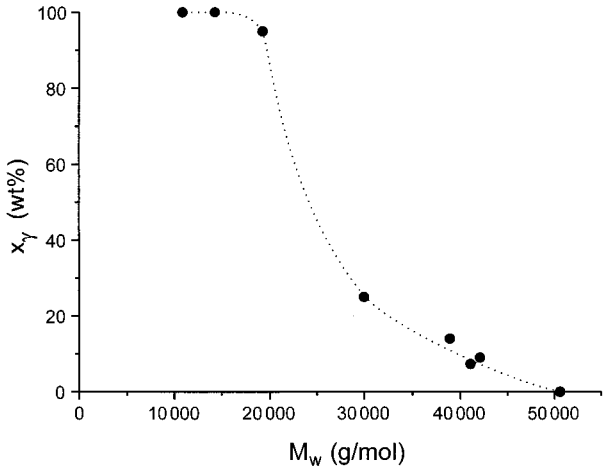

Figure 3. Fraction of γ-PDES as function of molecular weight.

β-PDES into the mesophase. The temperatures of this $\gamma \rightarrow$ i transition appeared to be rather independent of molecular weight. Obviously, the γ modification is less ordered, compared to β-PDES, as indicated by the lower heat of transition (Table 1). Figure 3 depicts the percentage of γ-PDES against molecular weight, as estimated from the peak areas. The coincidence of the critical molecular weight above which the mesophase is formed and the molecular weight below which mostly γ-PDES is found might suggest that γ-PDES is formed directly from the isotropic melt, while α- and β-PDES are formed from the mesophase. This would also explain why γ-PDES has its own distinct transition temperature. The enthalpy and entropy difference between the ordered crystalline state and the isotropic melt is overcome in one step for γ-PDES, instead of two steps for α- and β-PDES. Since $T = \Delta H/\Delta S$, it can not be expected that the γ melting transition evolves gradually from the $\alpha \rightarrow \mu$ or $\beta \rightarrow \mu$ transition.

For the higher molecular weights, the polymorphism can be affected by the cooling rate. If the sample is quenched from the melt, the α modification is formed predominantly. Slow cooling or annealing at the $\beta \rightarrow \mu$ transition results in pure β-PDES (Figure 4).

Figure 5 shows the enthalpies of the transition into the mesophase for the pure α and β polymorphs ($\Delta H_{\alpha \rightarrow \mu}$ and $\Delta H_{\beta \rightarrow \mu}$, respectively) as a function of molecular weight. Whereas the values for $\Delta H_{\beta \rightarrow \mu}$ increase with increasing molecular weight, those for $\Delta H_{\alpha \rightarrow \mu}$ decrease. Assuming an extended chain conformation for β-PDES, its increasing stability may be explained by the increasing size of the lamellae upon increasing molecular weight. Because α-PDES is prepared by quenching from the melt, higher amounts of defects can be expected

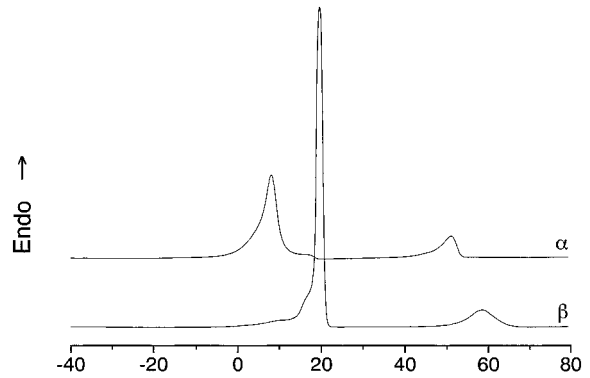

Figure 4. DSC heating scans for α-PDES (above, quenched from the melt) and β-PDES (below, crystallized from the mesophase at a rate of 2 °C/min, repeatedly followed by melting the residual α-PDES and cooling with 1 °C/min) (sample no. 9, heating rates 10 °C/min).

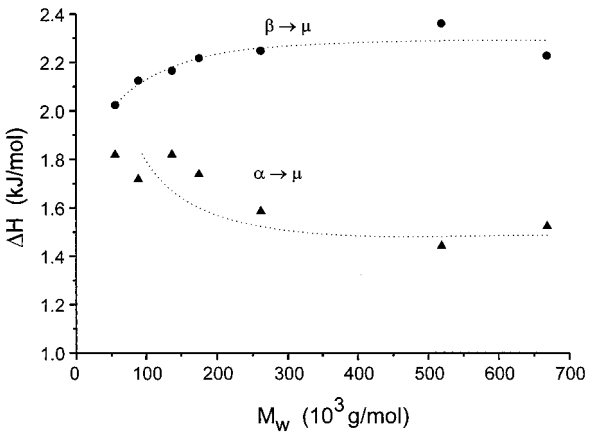

Figure 5. Transition enthalpies of pure α- and β-PDES vs molecular weight.

Table 2. PDES Transition Enthalpies and Entropies[a]

transition	ΔH (kJ/mol)	ΔS (J/mol·K)
$\gamma \rightarrow$ i	1.50 ± 0.04	5.66 ± 0.08
$\alpha \rightarrow \mu$[b]	1.51 ± 0.07	5.4 ± 0.26
$\beta \rightarrow \mu$[b]	2.27 ± 0.06	7.8 ± 0.20
$\mu \rightarrow$ i[b]	0.34 ± 0.01	1.07 ± 0.04

[a] Calculated per mole of repeating units. [b] High molecular weight samples.

in the crystals of higher molecular weight (i.e. less mobile) polymer chains. This is also reflected in the stability of the mesophase (Figure 4). In the case of a high molecular weight polymer (no. 9), the mesophase that is formed from β-PDES has a significantly higher melting point than the mesophase formed from α-PDES (T_i = 58.4 vs 52.7 °C). The same holds for the isotropization enthalpy (ΔH_i = 4.1 vs 3.3 J/g). For a lower molecular weight polymer (no. 4) virtually no difference was observed. Table 2 lists the values for the transition enthalpies and entropies, calculated assuming equilibrium (i.e. $\Delta S = \Delta H/T$). The agreement with those collected in ref 28 is good. The results presented in Table 2 and Figure 2 also show, however, that the "recommended average" values for the transition temperatures, enthalpies, and entropies given in ref 28 are not meaningful. The temperatures are strongly molecular weight dependent and average entropies and enthalpies depend on the ratio between α- and β-PDES, and thus on the sample's thermal history. The values for the transition enthalpies and entropies show the same trend as the transition temperatures and demonstrate that the β crystals are the most stable and ordered crystals.

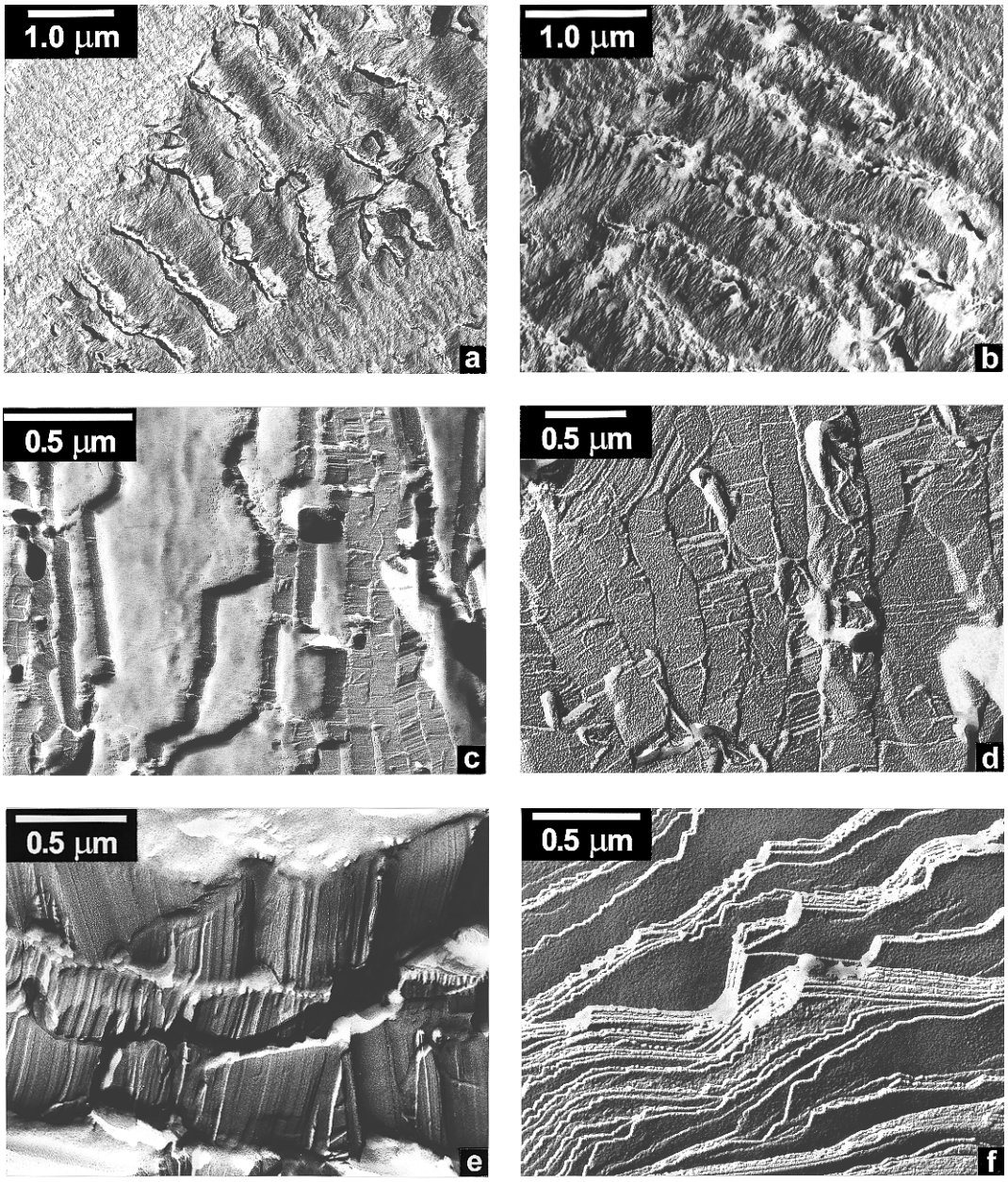

Figure 6. Electron micrographs of fracture surface replicas: (a) α-PDES no. 4; (b) α-PDES no. 7; (c) *β*-PDES no. 4; (d) *β*-PDES no. 7; (e) *β*-PDES no. 10; (f) *γ*-PDES no. 1 (thermal histories as described in the Experimental Section).

Two possible explanations exist for the molecular weight dependence of the isotropization temperature. *(i)* A melting point depression, due to the end groups is well-known for oligomers and causes a linear dependence of the reciprocal melting temperature $1/T_m$ from $1/M_n$:[27]

$$\frac{1}{T_m} = \frac{1}{T_m^{\,0}} + \frac{2R}{\Delta H_m n} \tag{1}$$

Here T_m^0 is the theoretical melting temperature of the polymer without end groups, R the gas constant, ΔH_m the melting enthalpy, and n the number average degree of polymerization. In the case of PDES, however, such an explanation has been discarded, because the isotropization enthalpy obtained according to eq 1 was an order of magnitude smaller than the experimentally obtained value.[10]

(ii) A better explanation, based on the assumption of an extended chain conformation of the macromolecules in the mesophase,[23] is the combination of the low enthalpy of isotropization ($\Delta H_i \approx 3$ J/g) and rather high values of the interfacial energy.[3,10] Assuming extended chain lamellar crystals, a simplified Gibbs−Tompson equation can be used to estimate the isotropization temperature T_i,[3] eq 2, where T_i^∞ is the isotropization

$$T_i = T_i^\infty\left(1 - \frac{2\sigma_e}{l\Delta H_i}\right) \tag{2}$$

temperature of a crystal of infinite thickness l, $\rho = 1.02$ g/cm^3 the density, $\Delta H_i = 3.3$ J/g the isotropization enthalpy, and σ the surface energy. The thickness of a lamella equals the length of an extended polymer chain, thus

$$l = \frac{c}{2}\frac{M_n}{M_0} \tag{3}$$

where $c = 4.88$ Å is the length along the chain axis of a unit cell containing two monomer units[2,3] and $M_0 = 102.2$, the molecular weight of one monomer unit. Combining eqs 2 and 3 and substituting the slope and

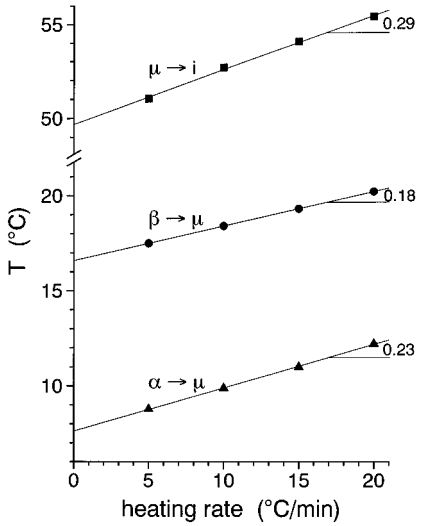

Figure 7. PDES transition temperatures as a function of the heating rate.

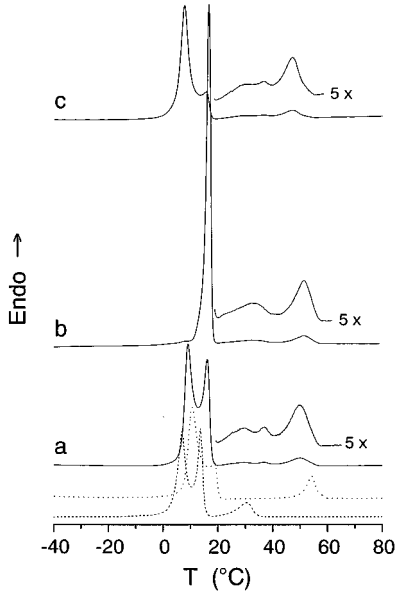

Figure 8. DSC heating scans for a bimodal PDES mixture (50 wt % no. 4 and 50 wt % no. 10) with different thermal histories: (a) after cooling from the melt with 10 °C/min (the broken lines indicate the DSC scans of both pure components); (b) after crystallizing from the melt with 1 °C/min, followed by repeated cycles of annealing at 13 °C and cooling with 0.5 °C/min; (c) after quenching from 100 °C (heating rates 10 °C/min).

$T_i^\infty = 326.1$ K, obtained from the linear fit in Figure 2, yield a value of $\sigma = 14.5 \times 10^{-3}$ J/m^2 for the surface energy, which agrees reasonably well with the value of 20×10^{-3} J/m^2, reported in ref 3.

Crystalline Morphology. Figure 6 shows electron micrographs of fracture surface replicas of α, β and γ-PDES. The micrographs that were obtained for the lower molecular weight β-PDES (no. 4, Figure 6c) show stacks of lamellae with a thickness of ca. 94 nm. The length of a stretched polymer chain, calculated from eq 3 with c = 4.72 Å,[2,3] amounts to $l = 120$ nm. For the higher molecular weight sample (no. 7, Figure 6d) similar structures with thicknesses around 300 nm were observed and $l = 320$ nm. However, the images depict thicker lamellae as well, which might indicate fusion of several thinner extended chain lamellae. Taking into account that the crystal surfaces are most likely not observed under an angle of exactly 90° and hence the thicknesses measured from TEM are accordingly too small, the agreement is good. For the highest molecular weight sample (no. 10, Figure 6e) lamellar thicknesses of ca. 600 nm were found, which is significantly lower than expected ($l = 1100$ nm). This might be ascribed to the broader molecular weight distributions and/or a less ordered packing, due to kinetic effects, in the case of very high molecular weights. As a consequence, the values for T_i^∞ and σ, as obtained from Figure 2 and eq 2, may be somewhat underestimated. γ-PDES (no. 1, Figure 6f) displays the same lamellar structure as the samples in the β phase. The lamellar thickness of ca. 28 nm corresponds very well with $l = 30$ nm, calculated for the length of a stretched polymer chain. In view of the evidence that the crystal structure of β- and γ-PDES resemble each other,[11,12] the differences in the heat of fusion might be explained by different degrees of crystallinity and possibly lower perfection of the γ crystals.

The samples in the α phase were much softer than β- and γ-PDES. Whereas the latter gave brittle fractures, freeze-fracturing α-PDES at −150 °C produced a surface that was partly cut and partly broken. The irregular structures that were typically observed at the broken surface (Figure 6a,b) are covered with bundles of chains in a much less orderly fashion than in the case of β- and γ-PDES.

Figure 7 shows the transition temperatures of a high molecular weight sample as a function of the heating rate. The heating rate dependence most likely depends on a complex number of factors and the absolute values for the slopes differ strongly per sample. Nevertheless, all samples show the same order in their heating rate dependencies: $\gamma \rightarrow$ i $\lesssim \beta \rightarrow \mu < \alpha \rightarrow \mu < \mu \rightarrow$ i. This demonstrates that the melting of γ-PDES and the $\beta \rightarrow \mu$ transition are the kinetically least complicated processes, and the melting of the mesophase is the kinetically most complicated process.

Influence of Molecular Weight Distribution. Figure 8 shows DSC heating scans for a 50/50 mixture by weight of a high molecular weight (no. 10) and a low molecular weight PDES sample (no. 4) with several different thermal histories. Figure 8a compares the heating scan after cooling from the melt with 10 °C/min with those of both components. The bimodal mixture showed two isotropization peaks that correspond to those of the pure components, shifted to slightly lower temperatures and in addition a third peak in between. This points to the existence of three types of mesophase crystals. The highest transition temperature can be assigned to the high molecular weight fraction. The inclusion of a small quantity of low molecular weight polymer would explain the somewhat lowered isotropization temperature. The lowest transition temperature belongs to the low molecular weight fraction, while the intermediate DSC peak may be caused by mixed crystals of the high and the low molecular weight portion. For both the $\alpha \rightarrow \mu$ and the $\beta \rightarrow \mu$ transition only one peak was observed, that lay between the peaks of the pure compounds and was somewhat broader, indicating a broader distribution of lamellar thicknesses. The signals were not split, because of the much weaker molecular weight dependence of the $\alpha \rightarrow \mu$ and $\beta \rightarrow \mu$ transition temperatures, compared to the isotropization temperature.

Figure 8b shows a DSC heating scan of the bimodal sample containing mostly the β polymorph. In this case, the middle isotropization peak had disappeared, indicating the presence of only two types of mesophase lamellae. Electron micrographs of fracture surface

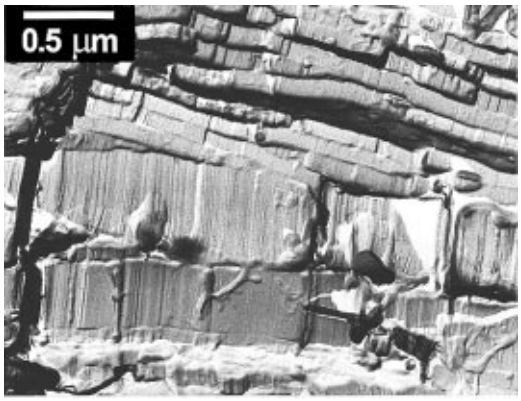

Figure 9. Electron micrographs of fracture surface replicas of bimodal β-PDES (50 wt % no. 4 and 50 wt % no. 10).

replicas of the same sample (Figure 9) confirmed this. Two types of lamellae were observed with thicknesses around 110 and 600 nm, respectively, corresponding very well with the thicknesses found for both pure components (Figure 6c,e).

A heating scan that was obtained after the sample had been quenched from 100 °C (Figure 8c) shows three isotropization peaks, which are somewhat broader than those in Figure 8a. DSC scans for a 50/50 mixture of PDES no. 4 and no. 8 were similar to Figure 8a−c. These results indicate a tendency of PDES for separation of the chains according to their length. The observation of a transition intermediate to those of the annealed sample can be regarded as an indication for the formation of mixed lamellae for the mesophase obtained from α-PDES. This points to a model for the structure of α-PDES where the packing of the chains is less ordered and chain ends are incorporated into the lamellae.

Conclusions

The good correlation between the lamellar thicknesses obtained from the TEM experiments and the calculated chain lengths have confirmed the extended chain conformation for β-PDES and demonstrated also an extended chain conformation for γ-PDES. When γ-PDES was heated, no mesophase was formed, which is most likely connected with the surface energy of the lamellae. The low heating rate dependence of the $\beta \rightarrow \mu$ transition and the linear relationship between isotropization temperature and reciprocal molecular weight indicate the existence of extended chain lamellae for the mesophase as well.

The chain-folded morphology that has been proposed for α-PDES[9] could not be confirmed. DSC experiments on bimodal PDES mixtures revealed a tendency for separation of the polymer chains according to their length. A number of observations point to a less ordered crystalline structure for α-PDES where chain ends are incorporated inside the crystals and no distinct lamellae are formed. These are *(i)* the greater softness, *(ii)* the lower stability of the α phase (lower values for $T_{\alpha\rightarrow\mu}$, $\Delta H_{\alpha\rightarrow\mu}$ and $\Delta S_{\alpha\rightarrow\mu}$) compared to the β phase, *(iii)* the higher heating rate dependence of the $\alpha \rightarrow \mu$ transition, and *(iv)* the fast exchange of ordered and less ordered molecular states observed before by NMR.[22]

Acknowledgment. Financial support was granted by the Deutsche Forschungsgemeinschaft (SFB 239, F3). R. Kulka (Universität Ulm, Sektion Elektronenmikroskopie) is thanked for his help in preparing the fracture surface replicas and Professor Yu. Godovsky for a valuable discussion.

References and Notes

(1) Papkov, V.; Godovsky, Yu.; Svistunov, V.; Litvinov, V.; Zhdanov, A. *J. Polym. Sci., Polym. Chem. Ed.* **1984**, *22*, 3617.
(2) Tsvankin, D.; Papkov, V.; Zhukov, V.; Godovsky, Yu.; Svistunov, V.; Zhdanov, A. *J. Polym. Sci., Polym. Chem. Ed.* **1985**, *23*, 1043.
(3) Godovsky, Yu.; Papkov, V. *Adv. Polym. Sci.* **1989**, *88*, 129.
(4) Möller, M.; Siffrin, S.; Kögler, G.; Oelfin, D. *Makromol. Chem., Macromol. Symp.* **1990**, *34*, 171.
(5) Out, G.; Turetskii, A.; Möller, M.; Oelfin, D. *Macromolecules* **1994**, *27*, 3310.
(6) Wunderlich, B.; Grebowicz, J. *Adv. Polym. Sci.* **1984**, *60/61*, 1.
(7) Wunderlich, B.; Möller, M.; Grebowicz, J.; Baur, H. *Adv. Polym. Sci.* **1988**, *87*, 1.
(8) Ungar, G. *Polymer* **1993**, *34*, 2050.
(9) Kögler, G.; Loufakis, K.; Möller, M. *Polymer* **1990**, *31*, 1538.
(10) Schlottke, H. Dissertation, Universität Mainz, Germany, 1995.
(11) Zavin, B.; Rabkina, A.; Kuteinikova, L.; Blagodatskikh, I.; Dubovik, I.; Gerasimov, M.; Papkov, V. *Vysokomol. Soed.* **1995**, *A37*, 507; *Polym. Sci.* **1995**, *A37*, 355.
(12) Out, G.; Turetskii, A.; Snijder, M.; Möller, M.; Papkov, V. *Polymer* **1995**, *36*, 3213.
(13) Froix, M.; Beatty, C.; Pochan, J.; Hinman, D. *J. Polym. Sci., Polym. Phys. Ed.* **1975**, *13*, 1269.
(14) Litvinov, V.; Lavrukhin, B.; Papkov, V.; Zhdanov, A. *Dokl. Akad. Nauk* **1983**, *271*, 900.
(15) Litvinov, V.; Lavrukhin, B.; Papkov, V.; Zhdanov, A. *Vysokomol. soed.* **1985**, *A27*, 1529; *Polym. Sci. USSR* **1985**, *27*, 1715.
(16) Siffrin, S. Dissertation, Universiteit Twente, Enschede, The Netherlands, 1993.
(17) Kögler, G.; Hasenhindl, A.; Möller, M. *Macromolecules* **1989**, *22*, 4190.
(18) Litvinov, V.; Whittaker, A.; Hagemeyer, A.; Spiess, H. *Colloid Polym. Sci.* **1989**, *267*, 681.
(19) Friedrich, J.; Rabolt, J. *Macromolecules* **1987**, *20*, 1975.
(20) Pochan, J.; Beatty, C.; Hinman, D.; Karasz, F. *J. Polym. Sci., Polym. Phys. Ed.* **1975**, *13*, 977.
(21) Miller, K.; Grebowicz, J.; Wesson, J.; Wunderlich, B. *Macromolecules* **1990**, *23*, 849.
(22) Grinberg, F.; Kimmich, R.; Möller, M.; Molenberg, A. *J. Chem. Phys.* **1996**, *105*, 9657.
(23) Papkov, V.; Svistunov, V.; Godovsky, Yu.; Zhdanov, A. *J. Polym. Sci., Polym. Phys. Ed.* **1987**, *25*, 1859.
(24) Hikosaka, M.; Rastogi, S.; Keller, A.; Kawabata, H. *J. Macromol. Sci.—Phys.* **1992**, *B31*, 87.
(25) Molenberg, A.; Siffrin, S.; Möller, M.; Boileau, S.; Teyssié, D. *Macromol. Symp.* **1996**, *102*, 199.
(26) Out, G.; Klok, H.; Möller, M.; Oelfin, D. *Macromol. Chem. Phys.* **1995**, *196*, 195.
(27) Flory, P. *Principles of Polymer Chemistry*; Cornell University Press, Ithaca, NY, 1953; p 570.
(28) Varma-Nair, M.; Wesson, J.; Wunderlich, B. *J. Therm. Anal.* **1989**, *35*, 1913.

MA970786U